F1 Car - Front Wing CFD Analysis and Optimization

J. Knapik[1], R.E. Gallyamov[2], V.A. Ovchinnikov[2], K.A. Volkova[3], E.V. Avdeev[4]

[1]Laduga Automotive Engineering, Spring Valley Road 145, Westerville, United States, 43081
[2]Laduga Automotive Engineering, Frunze 14B, Togliatti, Russia, 445037
[3]Peter the Great St. Petersburg Polytechnic University, Polytehnicheskaia 29, St. Petersburg, Russia, 195251
[4]Samara National Research University, Moskovskoe Shosse 34A, Samara, Russia, 443086

Abstract. This paper describes results of computational research of F1 car front wing design influence on drag and lift. Four different designs were proposed and investigated. Drag and lift coefficients of car, front and rear wings of different models were obtained. Conclusions on car's performance and further research were made.

Keywords: drag, lift, downforce, computational fluid dynamics.

1. Introduction
First racing cars were primarily designed to achieve high top speeds and the main goal was to minimize the air drag. But at high speeds, cars developed lift forces, which affected their stability. In order to improve their stability and handling, engineers mounted inverted wings profiles1 generating negative lift. First such cars were Opel's rocket powered RAK1 and RAK2 in 1928[1]. However, in Formula, wings were not used for another 30 years. Racing in this era occurred on tracks where the maximum speed could be attained over significant distance, so development aimed on reducing drag and potential of downforce had not been discovered until the late 1960's [2]. But since then, Formula 1 has led the way in innovative methods of generating downforce within ever more restrictive regulations.

2. Problem Statement
The purpose of current learning task is to investigate the effect of proposed front wing designs on drag and lift forces. Computational fluid dynamics (CFD) is used for simulation of open-wheel race-car movement in air at 142 mph. Car model and computational air domain are shown in the figure 1.

3. Race Car Aerodynamics

3.1. Types of Forces
While a vehicle is travelling at speed through a fluid (air) there are different types of forces will be acting upon the vehicle body. The process of vehicle movement related to surrounding air may be described as air flow at vehicle's speed in opposite direction around a stationary vehicle.

3.2. Aerodynamic Drag

Aerodynamic drag is the force that resists the movement of a body through a fluid medium. Aerodynamic drag varies with the square of the relative speed U between the vehicle and the surrounding air. When a vehicle travels through still air, doubling the vehicle speed approximately quadruples the aerodynamic drag.

In the presence of terrestrial winds that are not in-line with the vehicle motion, cross winds generate a non-zero yaw angle of the wind relative to the vehicle travel direction. For heavy-duty vehicles, such as tractor-trailer combinations, the drag coefficient increases significantly with yaw angle. The drag force on a vehicle may be calculated as follows [3]:

$$F_d = \frac{1}{2}\rho U^2 A C_d\left(\psi_\infty\right) \quad (1)$$

where F_d is the drag force, ρ is the density of the air, U is the speed of the object, relative to the surrounding air, ψ_∞ is the effective yaw-angle of the surrounding air relative to the vehicle motion, $C_d\left(\psi_\infty\right)$ is the drag coefficient which varies with yaw-angle, A is the projected frontal area of the vehicle.

To account for typical cross winds, a wind-average-drag coefficient can be defined that represents an average drag coefficient based on the predominant winds for a given region (typically an 11 km/hr (7 mph) wind speed in North America).

In (1) the drag coefficient is represented in a simple manner as a function of wind angle alone, shown as the function $C_d\left(\psi_\infty\right)$. In reality, the drag coefficient is a function of a number of factors related to the vehicle and the environment in which it operates [4].

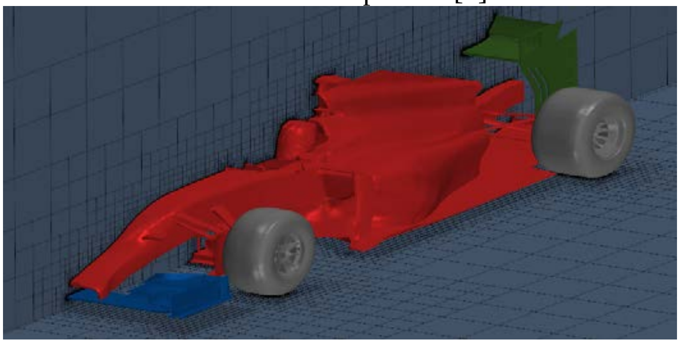

Figure 1. Car model and computational domain.

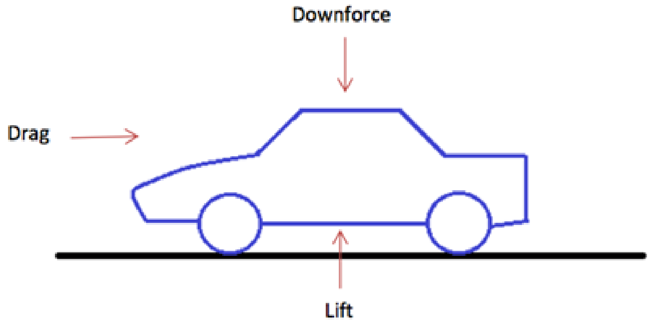

Figure 2. Diagram of forces.

There are two components of drag that affect a moving object [3]:

- Pressure Drag is the component of drag that acts in the direction of motion as a result of the pressure forces acting on the body.
- Friction Drag is the component of drag that acts parallel to a surface as a result of shear and viscous effects in the flow adjacent to the body surface.

3.3. Lift force

Lift is the components of the pressure and wall shear force in the direction normal to the flow tend to move the body in that direction. It can prevent the object from fly to the air when use the negative lift coefficient [5].

Lift force occurs according to 'Bernoulli Principle': when air travels at higher speed it creates lower pressure. The pressure difference between the top and bottom surface of the wing generate an upward force that tends the wing to lift. For the slender bodies such as wings, the shear force acts nearly parallel to the flow direction, thus its contribution to the lift is small. The lift force depend on the density, ρ, of the fluid, the upstream velocity U, the size, shape, and orientation of the body, among other things, and it is not practical to list these force for a variety of situations. Instead, it is found convenient to work with appropriate dimensionless numbers that present the drag and lift characteristics of the body. These numbers are the lift coefficient, C_L. It is defined as:

$$F_L = \frac{1}{2}\rho U^2 A C_L \tag{2}$$

where A is the frontal area of the body, $\frac{1}{2}\rho U^2$ is the dynamic pressure and F_L is lift force.

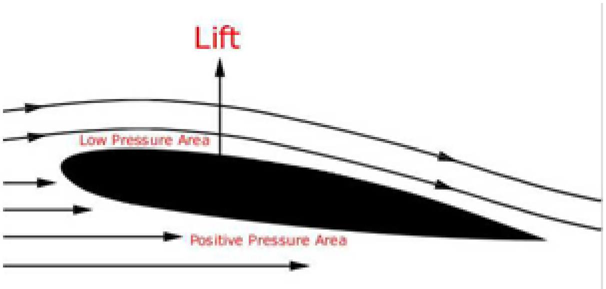

Figure 3. Lift direction.

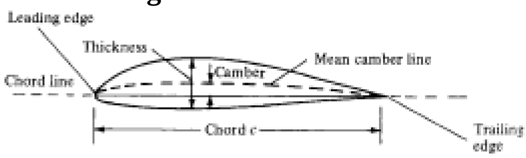

Figure 4. Airfoil nomenclature [3].

While race-car is moving - lift force creates instability. Motorsport is all about performance and specifically speed, in order to carry speed around corners the vehicle must have sufficient grip at the tires. In order to reach higher speeds car designers have to compensate lift force to increase stability. Downforce creates additional vertical load upon the tires relative to speed of vehicle. This allows the vehicle to travel as fast as possible around corners achieving the highest grip levels at the tires contact point.

The downside of the vehicle generating too much downforce is that drag forces will also increase which prevent the vehicle reaching the top speed when it is travelling in a straight line. So designing the body of vehicle it is important to control the flow around the car to generate the right amount of downforce [6].

There are different ways to control flow around the car which include designing front wings, spoilers, adding splitters and diffusers to generate higher speed of the air under the car.

3.4. Flow Over an Airfoil

Airfoil can be defined as a shape of wing, as seen in cross-section. In order to describe an airfoil, we must define the following term as seen in the figure 4 [3].

Concepts of drag and lift forces require to take into account viscous effect of the fluid (air). First, a boundary layer has to be admitted.

A boundary layer is a thin layer of viscous fluid close to the solid surface of a wall in contact with a moving stream in which (within its thickness δ) the flow velocity varies from zero at the wall (where the flow "sticks" to the wall because of its viscosity) up to U_e at the boundary, which approximately (within 1% error) corresponds to the free stream velocity (see figure 5). Strictly speaking, the value of δ is an arbitrary value because the friction force, depending on the molecular interaction between fluid and the solid body, decreases with the distance from the wall and becomes equal to zero at infinity [7].

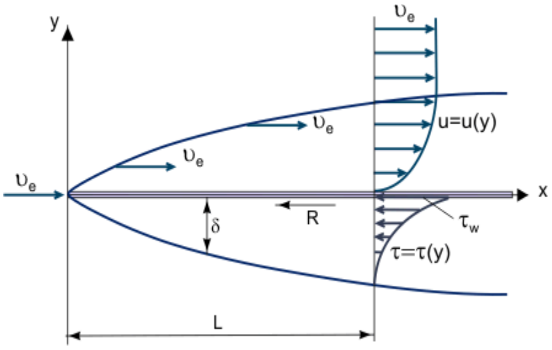

Figure 5. Growth of a boundary layer on a flat plate.

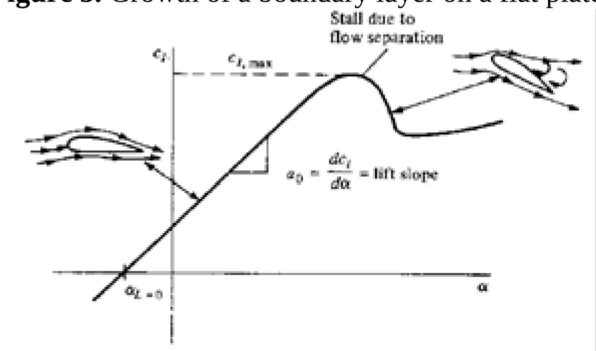

Figure 6. Variation of lift coefficient with the angle of attack.

The fundamental concept of the boundary layer was suggested by L. Prandtl (1904), it defines the boundary layer as a layer of fluid developing in flows with very high Reynolds Numbers R_e, that is with relatively low viscosity as compared with inertia forces. This is observed when bodies are exposed to high velocity air stream or when bodies are very large and the air stream velocity is moderate. In this case, in a relatively thin boundary layer, friction Shear Stress (viscous shearing force): $\tau = \eta\left[\partial u / \partial y\right]$ (where η is the dynamic viscosity; $u = u(y)$ – "profile" of the boundary layer longitudinal speed component, see figure 5) may be very large; in particular, at the wall where u = 0 and $\tau_w = \eta\left[\partial u / \partial y\right]_w$ although the viscosity itself may be rather small [3].

Another result of the viscous effect can be seen in the figure 6 which demonstrates variations of lift coefficient with the angle of attack. At low angles of attack c_l varies linearly with α, as predicted by the theory. However, at certain angle of attack, c_l reaches its maximum value $c_{l,\max}$ and starts to decrease. This is due to viscous effect of the air. First, the flow moves smoothly over the airfoil and is attached over most of the surface, but at certain value of α separates from the top surface, creating a wake of turbulent flow behind the airfoil, which results in drop in lift and increase in drag.

To increase lift of the airfoil, we must increase $c_{l,\max}$. As we have seen, the $c_{l,\max}$ of the airfoil primarily depends on its shape. Airfoil's shape can be changed with use of multielement flaps at the trailing edge and slats at leading edge. They increase chamber of the airfoil and therefore its $c_{l,\max}$ [8].

4. Computational Simulation Results

4.1. Initial F1 Model

The first part of the research was the obtaining of drag and lift coefficients for initial F1 car model. According to the “problem” appropriate boundary conditions were set as shown at figure 7. Air inlet velocity condition u = 142 mph was set at the frontal surface of computational domain; outlet condition was set at the opposite surface. Top, front and back sides of domain were described as symmetry boundary conditions. Also wheels rotation was settled at rotational frequency ω = 1900 rpm.

The results of the numerical solution for the initial F1 model are shown in Appendix A. Velocity and pressure distributions were obtained. Areas of high velocity can be observed under front and rear wings as shown at figure A.1. Hence, pressure in these areas is low which creates downforce acting on front and rear wings (see figure A.2)

Figure A.2 shows that low pressure area at the rear is much bigger than one near the front wing. Thus, it may lead to lower lift coefficient at the front wing. On the other hand figures also show that air flow behind the car is highly turbulent. Energy dissipation due to turbulence may increase drag coefficient at the rear wing comparing to the front wing.

Figure A.3 proves point about lesser downforce at the front wing. Higher static pressure was achieved on the rear wing which is even higher than static pressure on wheels’ surfaces that faces air stream directly. At the same time static pressure on the front wing is also high. Close look at the front wing is shown at figure A.4. Higher pressure occurs on the front edge of the wing. It can be explained by drag forces acting on the wing.

Additional figures of streamlines near front wing and pressure distribution for the initial F1 model can be found in Appendix A. The next step is to evaluate drag and lift coefficients. According to (1) drag coefficient C_d can be described as:

$$C_d = F_d / (\frac{1}{2}\rho U^2 A).$$

Lift coefficient can be obtained from (2) as follows:

$$C_L = F_L / (\frac{1}{2}\rho U^2 A).$$

The density at sea level will be assumed as no altitude was specified:

$$\rho = 1.2255 kg / m^3.$$

Projected frontal area of the vehicle is:

$$A = 1.295 m^2.$$

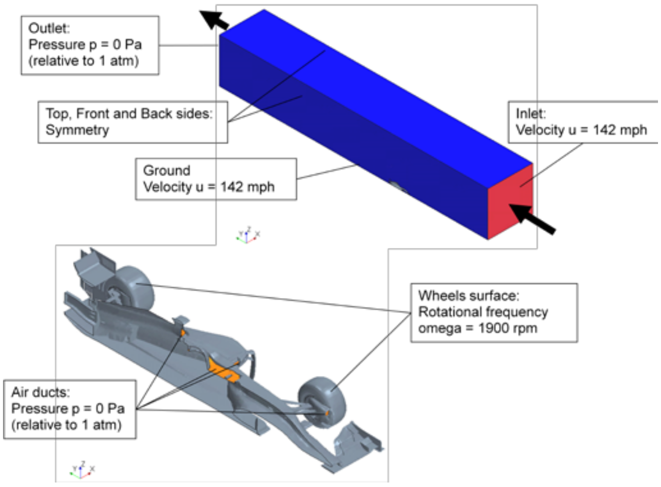

Figure 7. Boundary Conditions.

Vehicle velocity is equal to:

$U = 142 mph = 63.48 m/s$.

Drag force was obtained during solution and is equal to the component of force which acts on the vehicle or its part in the positive Y direction according to domain's coordinate system:

$F_d = 2334 N$.

Drag coefficient of F1 initial model is equal to:

$$C_d = 2334 / \left(\frac{1}{2} \cdot 1.2255 \cdot 63.48^2 \cdot 1.295 \right) = 0.73.$$

Lift force is the component of force acting in the positive Z direction. As long as downforce prevails in force balance in Z direction lift force will always have negative value as well as lift coefficient. Lift force which acts on the initial F1 model is:

$F_L = -1992 N$.

Hence, lift coefficient of initial F1 model is equal to:

$$C_L = -1992 / \left(\frac{1}{2} \cdot 1.2255 \cdot 63.48^2 \cdot 1.295 \right) = -0.62.$$

Calculations above are used to evaluate drag and lift coefficients of the front and rear wings. Projected frontal area of the front wing is:

$A_F = 0.154 m^2$,

and frontal area of the rear wing is:

$A_R = 0.174 m^2$.

Drag and lift forces acting on the front wing are respectively:

$F_{dF} = 256 N, \qquad F_{LF} = -1146 N$.

The rear wing is subjected by drag and lift forces of value:

$F_{dR} = 550 N, \qquad F_{LR} = -2060 N$.

Accordingly drag and lift coefficients of the front wing are:

$$C_{dF} = 256 / \left(\frac{1}{2} \cdot 1.2255 \cdot 63.48^2 \cdot 0.154 \right) = 0.67,$$

$$C_{LF} = -1146 / \left(\frac{1}{2} \cdot 1.2255 \cdot 63.48^2 \cdot 0.154 \right) = -3.01.$$

For the rear wing these values are:

$$C_{dF} = 550 / \left(\frac{1}{2} \cdot 1.2255 \cdot 63.48^2 \cdot 0.174 \right) = 1.28,$$

$$C_{LF} = -2060 / \left(\frac{1}{2} \cdot 1.2255 \cdot 63.48^2 \cdot 0.174 \right) = -4.8.$$

All the results are generalized in the Table I. As was predicted lift coefficient of the rear wing is much lower that of the front wing which means that downforce acting on the rear is higher. As the result the imbalance of downforce occurs. Still, the front wing is more efficient in the meaning of lift/drag relation. It happens because of much smoother air flow behind front wing than behind the rear wing.

As long as major reason of high drag coefficient of the rear wing is the high turbulence behind the car in general, all the efforts of the improvement of the initial car design should be focused on the increasing of lift coefficient of the front wing. It will lead to more balanced distribution of the downforce between front and rear wings.

4.2. Modified F1 Models

Four different designs of the front wing were chosen in order to optimize front wing designof this project. Simulations of the modified car models movement were held under boundary conditions described before.

Williams F1-2015 front wing design [8] was chosen as the first option. It is shown in the figure 8. All the results related to this design can be found in Appendix B.

The second chosen option was Mercedes F1-2015 front wing design [9] which is shown in the figure 9. Simulation results for that option are described in Appendix C.

Two modifications of the initial front wing plate were chosen as the third and fourth options. It was decided to change its original profile into airfoil. The airfoil Chuch Hollinger CH 10-48-13 smoothed (ch10sm-il) [10] was chosen as the third option and Eppler E420 (e420-il) [11] as the fourth option (see figure 10). All the data of airfoils profiles contains in UIUC Airfoil Coordinates Database [10 & 11]. Solution results for the third and fourth options are shown in Appendix D and Appendix E respectively.

Comparison of pressure distribution of different front wing designs shows that Williams and Mercedes designs do not create significant pressure difference which will affect downforce on the front wing. CH10-SM and E420 front wing plate designs demonstrate much bigger pressure difference in the front wing area.

Table 1. Results of the initial F1 model simulation.

Variable	Car Body	Front Wing	Rear Wing
Drag Coefficient	0.73	0.67	1.28
Lift Coefficient	-0.62	-3.01	-4.8
Efficiency (Lift/Drag)	0.853	4.477	3.745
% Force Z (Aero-balance)		38.6	61.4

Overall car body static pressure doesn’t have significant changes with different modifications. The front wing Williams and Mercedes designs demonstrate high static pressure at side wing plates - but static pressure on the main wing plate is near zero. Taking into account that the main plate has relatively high surface, downforce increasing at side wings will not affect overall front wing downforce toomuch.

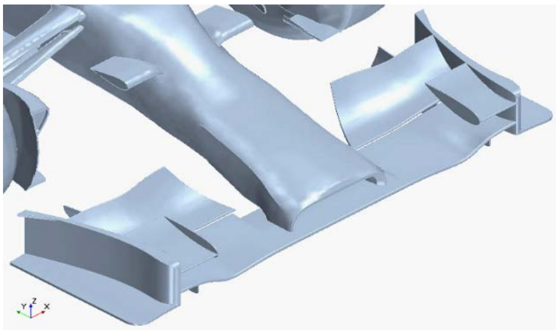

Figure 8. Option 1 - Williams F1-2015 Front Wing.

Changes in air flow produced by modified front wings also affect the air stream around car body. It may lead to increasing of the drag force due to more turbulent flow as can be seen from streamlines. Analysis of the pressure iso-surfaces around the front wing and car body shows that some disturbance in the stream has been occurred. However, more precise conclusion on the effect of the modified front wing designs can be made only by calculation of drag and lift coefficients.

Evaluation sequences of obtaining drag and lift coefficients as well as lift/drag efficiency and aero-balance for modified front wing designs are the same as for initial front wing design. Forces acting on car, rear and front wings for different options are shown in the Table II.

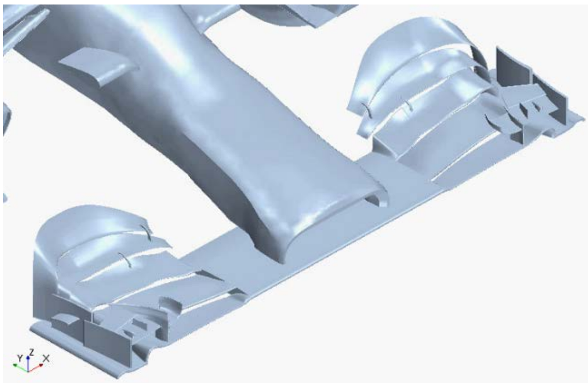

Figure 9. Option 2 - Mercedes F1-2015 Front Wing.

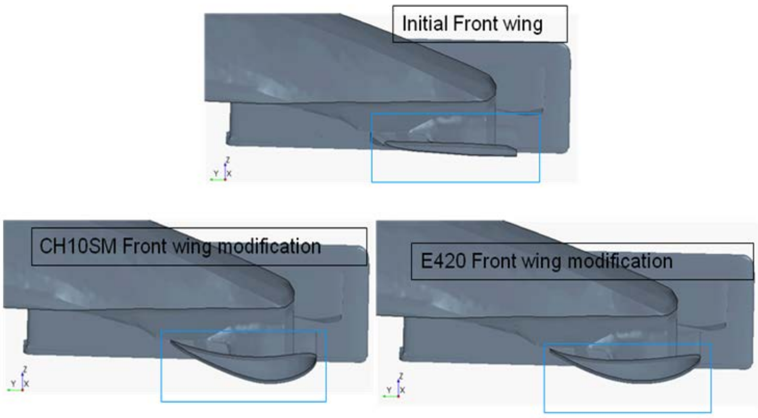

Figure 10. Options 3 & 4.

Results of drag and lift coefficients evaluation for all described models are shown in the Table III. The final comparison of all models efficiency and aero-balance are shown in the Table IV.

Table 2. Drag and Lift Forces Acting on Modified Car Designs.

Variable	Front Wing Design			
	Williams	Mercedes	CH10-SM	E420
Car Body Drag Force	2530	2530	2456	2462
Car Body Lift Force	-2054	-2060	-2410	-2488
Front Wing Drag Force	300	260	246	282
Front Wing Lift Force	-1422	-1202	-1938	-2000
Rear Wing Drag Force	520	592	556	540
Rear Wing Lift Force	-2040	-2082	-2064	-2064

Table 3. Drag and Lift Forces Acting on Modified Car Designs.

Variable	Front Wing Design				
	Initial Model	Williams	Mercedes	CH10-SM	E420
Car Body Drag Coefficient	0.73	0.79	0.79	0.77	0.77
Car Body Lift Coefficient	-0.62	-0.64	-0.67	-0.75	-0.78
Front Wing Drag Coefficient	0.67	0.7	0.75	0.65	0.74
Front Wing Lift Coefficient	-3.01	-3.31	-3.45	-5.07	-5.24
Rear Wing Drag Coefficient	1.28	1.21	1.38	1.3	1.26
Rear Wing Lift Coefficient	-4.8	-4.75	-4.85	-4.8	-4.8

Table 4. Efficiency and Aero-balance of Different Car Designs.

Variable	Front Wing Design				
	Initial Model	Williams	Mercedes	CH10-SM	E420
Car Body Efficiency (Lift/Drag)	0.853	0.813	0.848	0.98	1.01
Front Wing Efficiency (Lift/Drag)	4.477	4.731	4.62	7.867	7.077
Rear Wing Efficiency (Lift/Drag)	3.745	3.916	3.519	3.707	3.818
Front Wing % Force Z (Aero-balance)	38.6	54.0	42.5	62.7	64.6
Rear Wing % Force Z (Aero-balance)	61.4	46.0	57.5	37.3	35.6

It is clear from Tables III and IV that modification of the front wing also affects car body and rear wing drag and lift coefficients due to the changing of air flow conditions after the front wing area. However these changes are minor. In general, increasing of the downforce on the front wing leads to more unstable flow after it and causes increasing of the drag force on the car body.

All of the modified designs of the front wing show decreasing of the lift coefficient.

E420 wing plate design demonstrates the lowest lift coefficient. At the same time drag coefficient of this design is almost the highest among others (0.74 against 0.75 of Mercedes F1-2015 design). Still, efficiency of this design is rather high and takes the second place after CH10-SM wing plate design.

On the other hand, CH10-SM wing plate design shows the second best result according to lift coefficient but also demonstrates the lowest drag coefficient. Hence, it has the highest front wing efficiency among other designs (7.867).

While Mercedes F1-2015 design has the highest front wing drag coefficient its lift coefficient doesn’t really different from initial car design’s one. This design demonstrates the worst efficiency which even lower than efficiency of the initial front wing design.

Williams F1-2015 design decreases overall car efficiency but increases efficiency of the rear wing. It leads to the most balanced downforce distribution between front and rear wings.

5. Conclusion

The following results were obtained after computational simulation of movement of F1 car model with different front wing designs: Front wing plate with E420 airfoil profile shows the” best” overall car efficiency(lift vs.drag), and the “worst” front/rear aero-balance; while Front wing plate with CH10-SM airfoil profile shows the “best” front wing (lift /drag) efficiency.Williams F1-2015 modifications, on the other hand, shows the “best” rear wing efficiency and the “best” front/rear aero-balance. Finally, Mercedes F1-2015 front wing design shows the rear wing efficiency.

It may be concluded that the increasing of efficiency by using proposed Williams and Mercedes designs has not been significant in comparison to efficiency of two airfoil profiles(3 & 4), even though both designs show more balanced downforce distribution between front and rear wings.

While using of airfoils for a front wing profile for is very efficient in terms of downforce, without modifying of a rear wing it may lead to overall imbalance of downforce between front and rear wings. Further research should be focused on using airfoil as a front wing plate profile along with modification of the rear wing in order to decrease drag coefficient by stabilization of the air-flow behind the car and to improve aero-balance between front and rear wings. The existing car body also can be modified to become smoother which will lead to overall efficiency increasing. Additional efforts may be made in front wing design to deal with turning of air stream at front wheels. Maybe next focus should be also targeting testing of various ride heights or better understanding of wheel aerodynamics - the area of the greatest challenge, both experimentally and computationally [12].

In conclusion, any F1 aerodynamicist has two primary concerns: the creation of downforce, to help push the car's tires onto the track and improve cornering forces; and the mitigating drag - air resistance which acts to slow the car down. The “wings” on cars are often fitted with different profiles depending on many conditions and specific downforce needs of a particular race-track, making aerodynamic engineering and research even more challenging.

6. References

[1] Hucho, W.H. Aerodynamics of Road Vehicles, 4th edition / W.H. Hucho // Warrendale: Society of Automotive Engineers, 1998.
[2] Wright, P. Formula 1 Technology / P. Wright // Warrendale: Society of Automotive Engineers, 2001.
[3] Anderson, J.D. Fundamentals of Aerodynamics. 5th ed. / J.D. Anderson // Maidenhead: McGraw Hill Higher Education, 2010.
[4] Katz, J. Race Car Aerodynamics: Designing for Speed / J. Katz // Cambridge: Robert Bentley Publishing, 2006.
[5] Bertin, J.J. Aerodynamics for engineers / J.J. Bertin, R.M. Cummings, P. Venkata, H. Pearson, 2014.
[6] Pakkam, S.S. High Downforce Aerodynamics for Motorsports / S.S. Pakkam // M.Sc. Thesis Submitted to Graduate Faculty of North Carolina State University, North Carolina, 2011.
[7] Zhang, X. Aerodynamics of a Double Element Wing in Ground Effect / X. Zhang, J. Zerihan // AIAA Journal. – 2003. – Vol. 41(6). – P. 1007-1016.
[8] Williams F1-2015 front wing 3D model [Electronic resource]. – Access mode: https://grabcad.com/library/front-wing-f1-williams-team-1 (21.11.2017).
[9] Mercedes F1-2015 front wing 3D model [Electronic resource]. – Access mode: https://grabcad.com/library/f1-2015-front-wing-1 (21.11.2017).
[10] Airfoil Chuch Hollinger CH 10-48-13 smoothed (ch10sm-il) [Electronic resource]. – Access mode: http://airfoiltools.com/airfoil/details?airfoil=e420-il (21.11.2017).
[11] Airfoil Eppler E420 (e420-il) [Electronic resource]. – Access mode: http://airfoiltools.com/airfoil/details?airfoil=ch10sm-il (21.11.2017).